JOURNAL OF APPLIED ELECTROCHEMISTRY 22 (1992) 429–436

Free convective mass transfer at vertical cylindrical electrodes of varying aspect ratio

J. KRYSA

Department of Inorganic Technology, Prague Institute of Chemical Technology, 166 28 Prague 6, Czechoslovakia

A. A. WRAGG

School of Engineering, University of Exeter, North Park Road, Exeter EX4 4QF, UK

Received 23 July 1991; revised 2 October 1991

A limiting current technique was used for the measurement of the free convection mass transfer rate at entire vertical cylinders with varying aspect ratio. The mass transfer rates at the single surfaces were in good agreement with the mass transfer data in the literature. Mass transfer rates at a combination of a downward-facing horizontal and a vertical surface was controlled by the downward-facing horizontal surface (for cylinder aspect ratios lower than 2). It was found that the entire surface measured mass transfer rate was lower than that predicted by summation of the mass transfer rate at the individual surfaces. An interference factor, f, was introduced for correlation of the total mass transfer data for the full range of cylinders together. The dependence of the interference factor on the aspect ratio of the cylinder (L/r) was established.

Nomenclature

A_0	total surface area of cylinder
A_V	vertical surface area of cylinder
A_H	surface area of horizontal base of cylinder
c_b	bulk concentration of copper ion
c_{CuSo_4}	bulk concentration of copper sulphate
$c_{H_2SO_4}$	bulk concentration of sulphuric acid
d	cylinder diameter
D	diffusion coefficient of copper ion
f	interference factor
F	Faraday's constant
g	gravitational acceleration
I_L	limiting diffusion current
k	mass transfer coefficient
L	cylinder length
L_w	characteristic dimension (Weber *et al.* [2])
n	charge number of copper ion
r	cylinder radius
Ra	Rayleigh number
Ra_L	Rayleigh number based on cylinder length
Sh	Sherwood number
Sh_L	Sherwood number based on vertical cylinder length
Sh_0	stagnant medium Sherwood number
T	electrolyte temperature

Greek symbols

$\Delta\rho$	density difference between bulk solution and interface
ρ	density
μ	dynamic viscosity

1. Introduction

Much work has been done recently on natural convection heat and mass transfer processes. This reflects the growing importance of such processes in science and engineering and the environment. Unfortunately, very little has been done on the behaviour of three dimensional objects and there is still confusion concerning the best approach for correlation of data for such objects. In this work the electrochemical technique has been used to examine natural convection from cylindrical vertical cathodes. Correlations obtained from measured separate surface mass transfer coefficients were used for formation of the overall mass transfer correlation. The method takes account of the convective interaction between adjacent surfaces.

Previous work was undertaken by Selman and Attar [1] who studied free convection mass transfer to a rod shaped vertical electrode. The mass transfer rate to the horizontal (disc) face and the vertical (curved) face were measured separately and in combination. Selman and Attar found that the two rates are not additive because of the significant interaction caused by leading edge effects at the vertical face and by solution streaming from the horizontal to the vertical surface.

Weber *et al.* [2] measured and correlated natural convection heat and mass transfer from three dimensional objects, including spheres, cones, cylinders and cubes, as well as flat plates using the limiting current technique. The characteristic dimension for such

0021-891X/92

object was defined as

$$L_w = \frac{\text{Surface area}}{\text{Perimeter projected onto horizontal plane}} \quad (1)$$

Weber *et al.* [2] obtained the universal correlation

$$Sh - Sh_0 = 0.53\,(RaF(Sc))^{0.256} \quad (2)$$

where

$$F(Sc) = \left[1 + \left(\frac{0.5}{Sc}\right)^{4/16}\right]^{-16/9} \quad (3)$$

and Sh_0 represents the purely diffusive Sherwood number in still fluid.

Sedahmed and Nirdosh [3] investigated free convection mass transfer at horizontal cylinders with active ends. The characteristic length used in the calculation of *Sh* and *Gr* was obtained by dividing the surface area of the cylinder by the perimeter projected onto the horizontal plane [2]. Data were correlated by the equation

$$Sh = 0.32\,(Gr\,Sc)^{0.28} \quad (4)$$

in the range $2.3 \times 10^8 < Gr\,Sc < 1.7 \times 10^{11}$.

Worthington *et al.* [4], in an investigation to model natural convection heat dissipation from electronic components, studied electrochemical mass transfer at horizontally oriented cuboids and found that the overall measured rate of mass transfer was lower than the value predicted by summing the rates of mass transfer at the different individual faces. This led the authors to use a correction factor termed, 'interference factor'. The authors attribute the discrepancy between the predicted and experimental rates of mass transfer to the fact that the sides and top are exposed to fluid that has already been depleted of the transferred ion at the bottom surface of the cuboid. The objective of the present work was to measure the mass transfer rates at vertical cyclinders of varying aspect ratio and to seek an effective overall correlation method.

2. Experimental details and procedure

The experiments were performed in a cylindrical 5 dm^3 glass container of internal diameter 16 cm and height 23 cm. Copper sulphate concentration varied from 0.01 to 0.23 M which, with cylinder length as characteristic dimension, gave Rayleigh numbers between 2.12×10^5 and 1.3×10^{11}. Each solution contained 1.5 M sulphuric acid as the supporting electrolyte. The electrolyte temperature was carefully measured and always lay within the range 18–20° C being constant to +0.1° C during each individual experiment. The cylindrical electrodes were milled from solid copper, then lapped and polished and finishing with 1200 grade wet and dry abrasive paper. Each electrode was supported using a 1 mm diameter copper wire glued into a hole in the centre of the top of each cylinder. This wire also served as current carrier. The wire was lacquered to insulate it from the electrolyte. The vertical copper cylinder cathodes were placed in the centre of the container midway between the top and the bottom of the solution. A cylindrical copper mesh of diameter 16 cm and height 23 cm was used as an anode. The arrangement of the apparatus is shown in the Fig. 1.

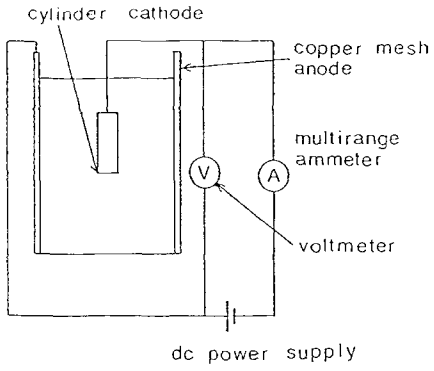

Fig. 1. Diagram of cell and electrical circuit.

The actual Cu^{2+} concentration was periodically determined by spectrophotometric analysis. The usual electrical circuit for limiting current measurement was employed, consisting of a d.c. power supply with a voltage regulator, a high impedance voltmeter and a multirange ammeter. Limiting currents were obtained by an experimental procedure, which has been reported in detail previously [5]. The anode acted as a reference electrode in view of its high area compared to that of the cathode. Under such conditions polarization is negligible at the anode and the cell current–voltage relation depends only on the conditions prevailing at the cathode. The onset of the limiting current was well defined and reproducible.

Table 1 lists all the dimension of the cylinders used. This work considers only vertical cylinders with two horizontal surfaces and one vertical surface. All cylinders were of 2 cm diameter. In this investigation L ranged from 0.2 to 15 cm. The mass transfer limiting currents to the vertical surface and to the upward-facing and downward-facing horizontal surfaces were measured separately and in combination, e.g. to the cylinder with active vertical and downward-facing surfaces and to the entire cylinders with active ends. Table 1 summarizes the geometric parameters of the electrodes with the characteristic length L_w as defined by Weber *et al.* [2] (Equation 1).

*Table 1. Electrode geometries**

Electrode	*L*/cm	A_0/cm^2	A_V/cm^2	A_H/cm^2	A_V/A_H	L_w/cm
1	0.2	7.54	1.26	3.14	0.4	1.2
2	0.5	9.42	3.14	3.14	1.0	1.5
3	1.0	12.56	6.28	3.14	2.0	2.0
4	3.0	25.13	18.85	3.14	6.0	4.0
5	5.0	37.70	31.40	3.14	10.0	6.0
6	15.0	100.55	94.40	3.14	30.0	16.0

* Cylinder diameter is 2 cm in all cases.

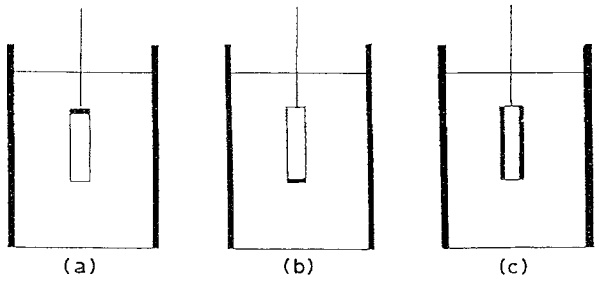

Fig. 2. Geometry of the electrodes in separate mass transfer measurement. (a) upward-facing horizontal surface, (b) downward-facing horizontal surface, and (c) vertical surface; black-active electrode surface, white-isolation.

3. Results and discussion

3.1. *Mass transfer data calculation*

The data were expressed in terms of the Sherwood number

$$Sh = kL/D \tag{5}$$

and mass transfer Rayleigh number

$$Ra = g\Delta\rho L^3/\mu D \tag{6}$$

The mass transfer coefficient, k, was calculated using the relation

$$k = I_L/A_0 nFc_b \tag{7}$$

The area in this equation was the total available for mass transfer at the electrode. The correction for the attachment of the supporting wire was small, never being more than 1% of the exposed area. The diffusivity of the Cu^{2+} ion was calculated using the equation

$$\mu D/T = (2.495 + 0.0173c_{CuSO_4} + 0.0692c_{H_2SO_4}) \times 10^{-15}\,\mathrm{N\,K^{-1}} \tag{8}$$

due to Fenech and Tobias [6]. This equation was used in preference to the more recent one of Selman and Tavakoli-Attar [1] as the temperature of the solutions in this investigation were closer to those used by Fenech and Tobias. Density and viscosity were calculated using data of Eisenberg *et al.* [7]. The $\Delta\rho$ terms were taken from Wilke [13]. The effect of migration on the copper deposition rate was negligible; the migration contribution for the highest concentration of copper sulphate (0.231 M) was 1.5% [8]. Values of Sh_0 were subtracted from the overall Sherwood number leaving the convection component of the overall transfer rate. Values of Sh_0 were calculated using the method presented by Clift *et al.* [16] according to the equation

$$Sh_0 = k_0 L/D = \frac{8 + 6.95(L/d)^{0.76}}{2\pi} \tag{9}$$

Values of Sh_0 are given in Table 2.

3.2. *Single active surface*

The geometry of the electrodes used in the measurement of free convection mass transfer at the downward and upward-facing horizontal and vertical surfaces separately are described in Fig. 2. The convection relating to the limiting current at the downward-facing horizontal surface involves an upward escape of light solution, depleted in $CuSO_4$, around the edge of the exposed disc surface. This convection is an example of bulk flow streaming induced by buoyancy similar to that investigated by Fenech [9], Wragg

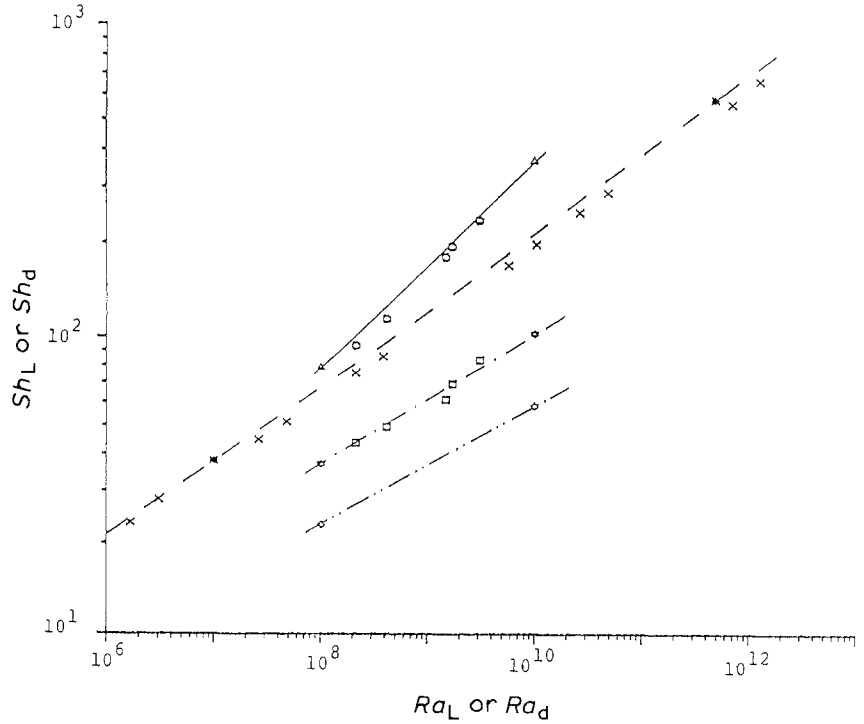

Fig. 3. Separate surface mass transfer correlation for (a) upward-facing horizontal surface, (b) downward-facing horizontal surface, and (c) vertical surface. Experimental values: (a) ○, (b) □, (c) ×; literature values: (a) –△– [12], (b) ··◇·· [14] –·☆·– [15], —∗— [13].

Table 2.

Cylinder	1	2	3	4	5	6
Sh_0	1.47	1.67	1.93	2.78	3.49	6.39

et al. [10], Selman *et al.* [1] and White [11] adjacent to a horizontal electrode. The influence of the edge of the active surface is more significant when the disc diameter is smaller. A plot of *Sh* against *Ra* is shown as Fig. 3 and comparison is made with the Fujii *et al.* [14] downward-facing surface data in heat transfer, and also with the equation of Loomba [15] for electrochemical mass transfer at down-facing discs. The present results agree well with the data of Loomba [15]. The discrepancy between the present data and the equation of Fujii *et al.* [14] is explained by fact that the data of Fujii were determined for a rectangular plane and the effect of the edge of a rectangular surface is less than that of a disc.

From Fig. 3 good agreement between the present data for upward-facing horizontal surfaces and those for other studies [12] is apparent. Results for mass transfer to the vertical cylindrical surface are also expressed in Fig. 3. There is very good agreement with the vertical plate mass transfer results of Wilke *et al.* [13], who produced the correlating equation

$$Sh = 0.673(Ra_L)^{0.25} \tag{10}$$

in the range $10^6 < Ra_L < 10^{12}$.

3.3. *An approach to correlation for active ended vertical cylinders*

By adding the mass transfer rates from correlations for the separate sides a total mass transfer performance can be predicted. The advantages of this method are discussed in [4]. In the present approach the correlation for the vertical surface was taken from Wilke *et al.* [13]. For the upward-facing horizontal surface the correlation of Patrick *et al.* [12] was used. The correlation used in the prediction for the downward-facing horizontal surface was derived from results of Loomba [15]. The mass transfer rates for separate surfaces were correlated by using cylinder diameter [12], [15] and cylinder length [13] as characteristic dimensions. The resultant predicted natural convection mass transfer rate for a vertical cylinder then becomes

$$Sh_L - Sh_0 = \left(\frac{0.72r + 1.34L + 0.64rRa_L^{-0.03}}{2L + 2r}\right) Ra_L^{0.25} \tag{11}$$

in the laminar region $10^4 < Ra_L < 8 \times 10^6$.

For Rayleigh numbers greater than 8×10^6 there is a transition to turbulence over the upward-facing horizontal surface. Using the individual surface summation approach for this regime gives

$$Sh_L - Sh_0 = \left(\frac{0.17rRa_L^{1/12} + 1.34L + 0.64rRa_L^{-0.03}}{2L + 2r}\right) Ra_L^{0.25} \tag{12}$$

where L and r are the vertical cylinder length and cylinder radius and Ra_L is the mass transfer Rayleigh number based on the vertical dimension of the cylinder.

The mass transfer performance for the whole cylinder active was measured with a view to evaluating the usefulness of Equation 12.

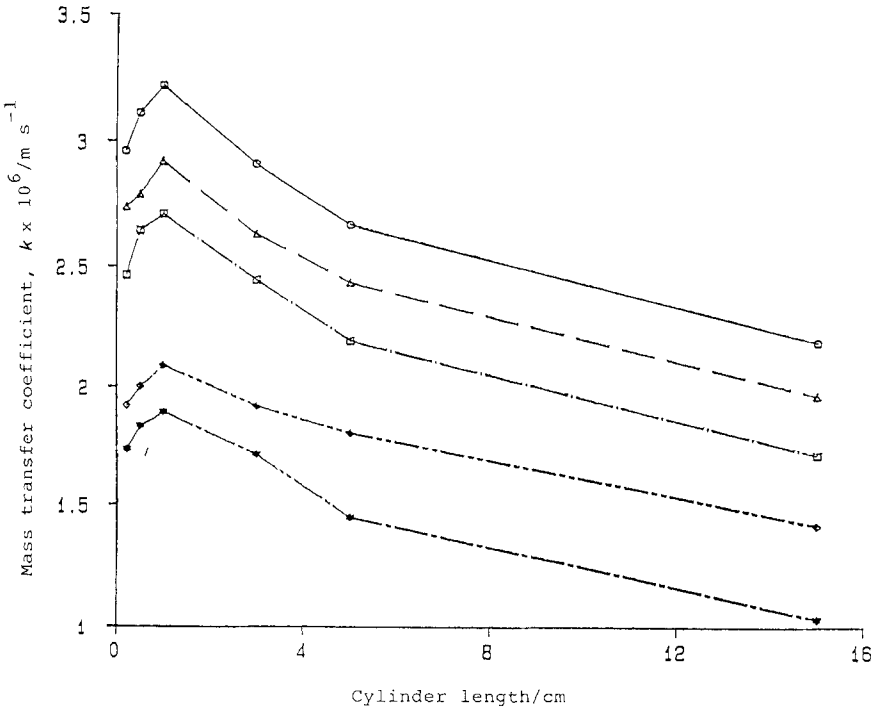

Fig. 4. The effect of cylinder length on mass transfer coefficient for a combination of down-facing horizontal surface and vertical surface for five different concentrations of copper sulphate: (○) 0.231, (△) 0.129, (□) 0.111, (◇) 0.031 and (*) 0.016 M.

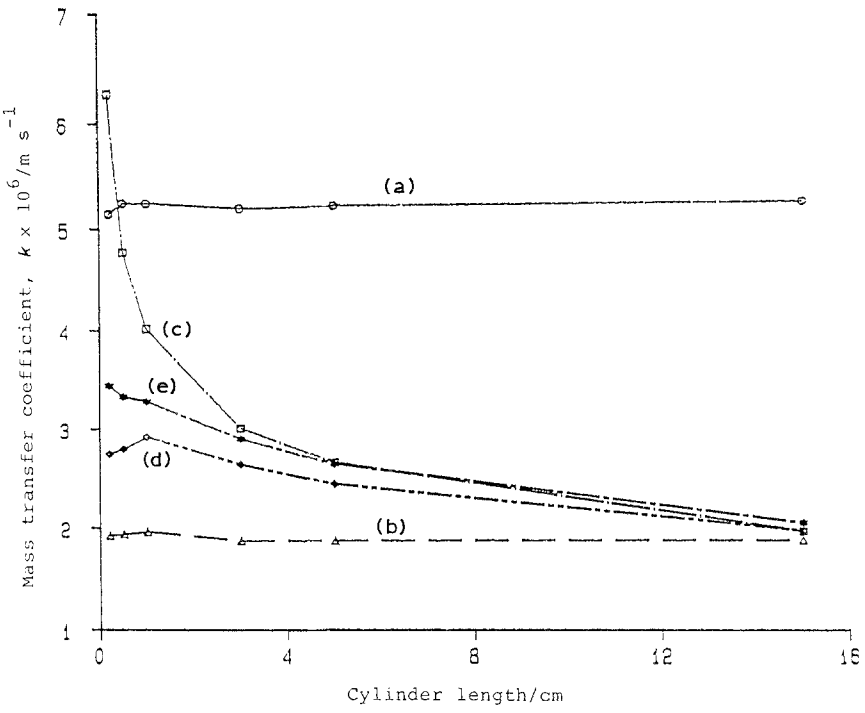

Fig. 5. The effect of cylinder length on mass transfer coefficient for different surfaces for a single concentration of copper sulphate, $c = 0.129$ M. (a) Upward-facing horizontal surface, (b) downward-facing horizontal surface, (c) vertical surface, (d) combination of downward-facing horizontal surface and vertical surface, and (e) total surface. (a) ○, (b) △, (c) □, (d) ◇ and (e) ∗.

3.4. *Mass transfer at combinations of surfaces*

Mass transfer coefficients for the simultaneously active vertical cylinder surface and the downward-facing horizontal surface for different cylinder lengths are shown in Fig. 4. The results show that the mass transfer rate is crucially dependent on the vertical to downward-facing horizontal surface dimension ratio. For cylinders with ratio lower than 2 the mass transfer coefficients are controlled by the downward horizontal surface. This causes decreasing values of mass transfer coefficients with surface aspect ratio (A_0/A_H) 0.4 and 1 whereas for a vertical surface k approaches ∞ as L becomes small.

Mass transfer coefficients for the separate surfaces and for the surfaces in combination are plotted in

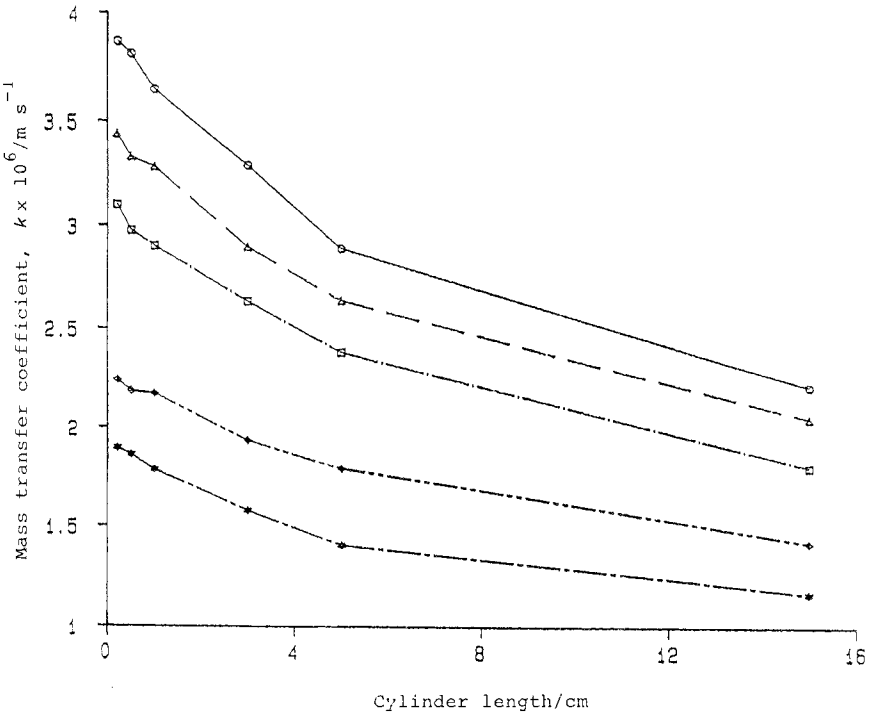

Fig. 6. The effect of cylinder length on overall mass transfer coefficient for five different concentrations of copper sulphate: (○) 0.231, (△) 0.129, (□) 0.111, (◇) 0.031 and (∗) 0.016 M.

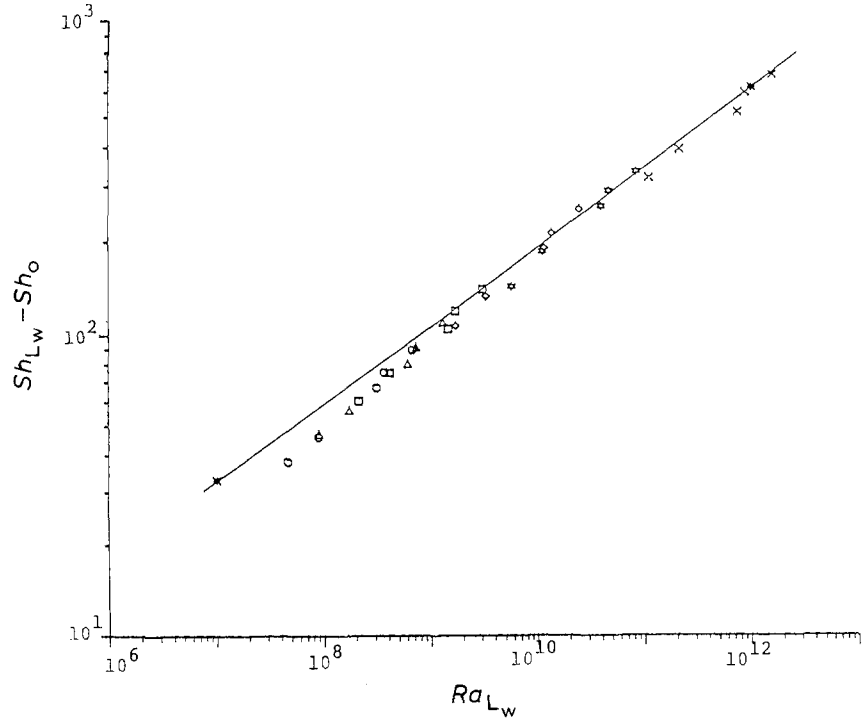

Fig. 7. Correlation of cylinder mass transfer data using the Weber *et al.* [2] characteristic dimension. Cylinders: (○) 1, (△) 2, (□) 3, (◇) 4, (☆) 5 and (×) 6. Correlation of Weber *et al.* [2] (Equation 2).

Fig. 5 for a single concentration of copper sulphate (0.129 M).

The effect of cylinder length, L, on the mean mass transfer coefficient for the total surface is shown in Fig. 6.

For higher vertical to horizontal surface dimension ratios (3 and more) the vertical surface controls the mass transfer behaviour but there is distinct departure from the vertical surface behaviour (Fig. 5, curve C) for $L/r < 3$.

3.5. *Total correlation*

3.5.1. Weber dimension approach. The results from all the cylinders are plotted using the characteristic length defined by Weber *et al.* [2] in Fig. 7. The correlation of Weber *et al.* (Equation 2), which was derived using objects of many different shapes is also shown. It is seen that the data from all the present cylinders lie below the Weber correlation with deviation of up to 20%. This may be explained by

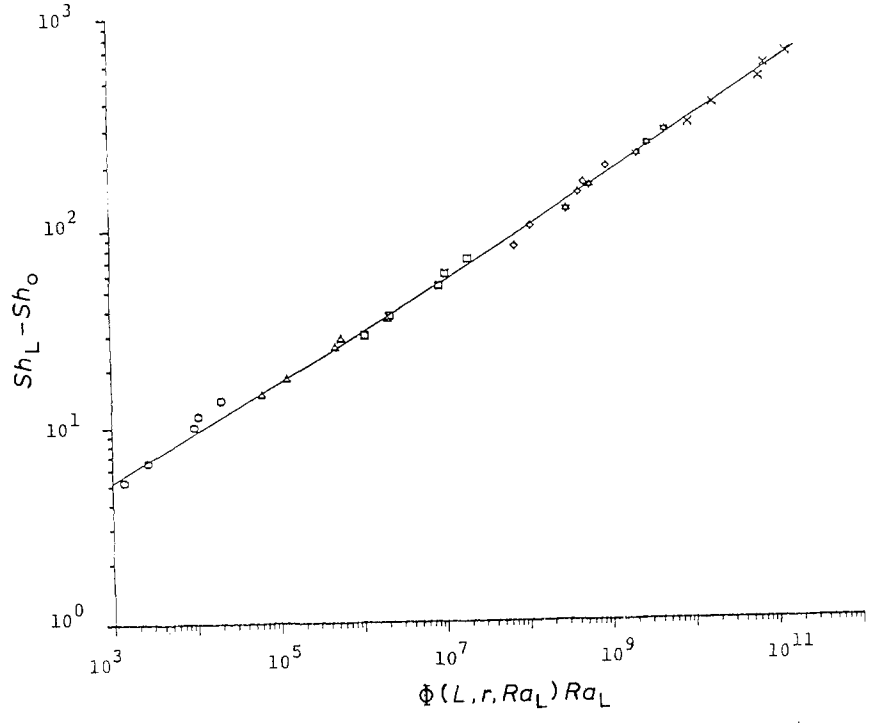

Fig. 8. Correlation of whole cylinder data in terms of Equation 13. Cylinders as in Fig. 7.

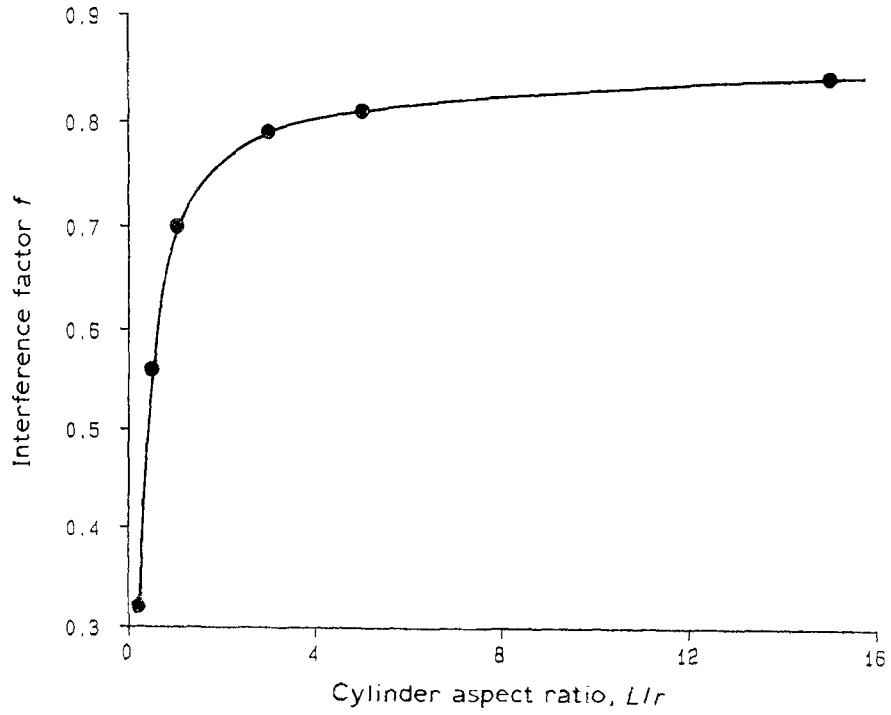

Fig. 9. Plot showing variation of interference factor f with cylinder aspect ratio L/r.

the fact that the relatively inactive down-facing horizontal surface reduces the overall mass transfer rate. The Weber correlation was obtained for objects not having this surface, e.g. horizontal cylinders, spheres, cones. Worthington *et al.* observed the same discrepancy when correlating natural correlation mass transfer to cuboids using the Weber approach.

3.5.2. Separate side approach. The behaviour predicted by Equations 11 and 12 was compared with the mass transfer data for all the cylinders. It was found in every case that the predicted rate was higher than the actual data but that the shape and gradient of the prediction and results were well matched. The flow of the fluid around the cylinder base and up the vertical surface means that the vertical and upward-facing horizontal surfaces are exposed to solution which has already been depleted of copper ions. Thus the overall mass transfer rate for a cylinder is lower than that for the equivalent summed separate surfaces (see Fig. 5). A multiplying factor f, may be introduced to Equations 11 and 12, to represent the lower rate of mass transfer at the vertical and upward-facing horizontal surfaces. Measurements at the upward horizontal surface indicates that the transition to turbulent flow has occurred for all cylinders (see Fig. 3). The multiplying factor, f, is therefore only used to modify the rate of mass transfer in Equation 12. This equation now becomes

$$Sh_L - Sh_0 = \left(\frac{f(0.17rRa_L^{1/12} + 1.34L) + 0.64rRa_L^{-0.03}}{2L + 2r}\right) Ra_L^{0.25} \quad (13)$$

for turbulent flow.

Values of f were obtained from Equation 13 and calculated for each cylinder. These are tabulated in Table 3. f varies between 0.84 for the tallest cylinder and 0.32 for the smallest cylinder.

$Sh_L - Sh_0$ has been plotted to show data from all the cylinders against $\Phi(L, r, Ra_L)Ra_L$ in Fig. 8. $\Phi(L, r, Ra_L)$ is given by

$$\Phi(L, r, Ra_L) = \left(\frac{f(0.17rRa_L^{1/12} + 1.34L) + 0.64Ra_L^{-0.03}}{2L + 2r}\right)^4 \quad (14)$$

for turbulent flow.

It can be seen that all the data fit the line representing Equation 13 very well. All the points except one lie within a deviation +5% from the line and the fit is better than for the Weber correlation. Figure 9 shows the dependence of f on the cylinder aspect ratio (L/r). The plot shows that for low values of L/r (from 0.2 to 1) the interference factor f depends very strongly on L/r and for higher values of L/r (5 and more) it becomes constant.

Introduction of the curvature effect as described by Ravoo *et al.* [17] produces a modified Equation 13:

$$Sh_L - Sh_0 = \left(\frac{f(0.17rRa_L^{1/12} + 1.34L\Phi(\gamma)) + 0.64rRa_L^{-0.03}}{2L + 2r}\right) \times Ra_L^{0.25} \quad (15)$$

Table 3.

Cylinder	1	2	3	4	5	6
f	0.32	0.56	0.70	0.79	0.81	0.84

where

$$\gamma = (L/r)(Ra_L)^{-0.25} \quad (16)$$

At high Ra_L, or small L/r, γ is $\ll 1$ and $\Phi(\gamma) \to 1$. The practical limit for the absence of curvature effects is $\gamma = 0.2$ according to [17]. This value was not exceeded in the present work.

Acknowledgement

The authors wish to thank Dr. M. A. Patrick for helpful discussions regarding data treatment. The provision to JK of a mobility grant under the CEC TEMPUS programme is also gratefully acknowledged.

References

[1] J. R. Selman and J. Tavakoli-Attar, *J. Electrochem. Soc.* **127** (1980) 1049.
[2] M. E. Weber, P. Austraukas and S. Petsalis, *Can. J. Chem. Eng.* **62** (1984) 68.
[3] G. H. Sedahmed and I. Nirdosh, *Int. Comm. Heat Mass Transfer* **17** (1990) 355.
[4] D. G. Worthington, M. A. Patrick and A. A. Wragg, *Chem. Eng. Res. Des.* **65** (1987) 131.
[5] A. F. J. Smith and A. A. Wragg, *J. Appl. Electrochem.* **4** (1974) 21.
[6] E. J. Fenech and C. W. Tobias, *Electrochim. Acta* **2** (1960) 211.
[7] M. Eisenberg, C. W. Tobias and C. R. Wilke, *J. Electrochem. Soc.* **103** (1956) 413.
[8] N. Ibl and O. Dossenbach, *in* 'Comprehensive Treatise of Electrochemistry', vol. 6 (Edited by E. Yeager, J. O' M. Bockris, B. E. Conway and S. Sarangapani). Plenum Press, New York (1983) pp. 192–8.
[9] E. J. Fenech, Ph.D. Thesis, University of California, Berkeley, UCRL-9079 (1960).
[10] M. A. Patrick and A. A. Wragg, *Electrochim. Acta* **19** (1974) 929.
[11] G. M. L. White, Project Report, University of Exeter, Department of Chemical Engineering (1988).
[12] M. A. Patrick and A. A. Wragg, *Int. J. Heat Mass Transfer* **18** (1975) 1397.
[13] C. R. Wilke, C. W. Tobias and M. Eisenberg, *J. Electrochem. Soc.* **100** (1953) 513.
[14] T. Fujii and H. Imura, *Int. J. Heat Mass Transfer* **15** (1972) 755.
[15] R. P. Loomba, M.Sc. Thesis, University of Manchester Institute of Science & Technology (1969).
[16] R. Clift, J. R. Grace and M. E. Weber, 'Bubbles Drops and Particles', Academic Press, New York (1978) pp. 88–9.
[17] E. Ravoo, J. W. Rotte and J. W. Sevenstern, *Chem. Eng. Sci.* **25** (1970) 1637.